High-resolution study of the ^{9}Be(^{3}He,t)^{9}B reaction up to the ^{9}B triton threshold

C. Scholl, Y. Fujita, T. Adachi, P. von Brentano, H. Fujita, M. Górska, H. Hashimoto, K. Hatanaka, H. Matsubara, K. Nakanishi, T. Ohta, Y. Sakemi, Y. Shimbara, Y. Shimizu, Y. Tameshige, A. Tamii, M. Yosoi, and R. G. T. Zegers

Phys. Rev. C **84**, 014308 — Published 12 July 2011

DOI: 10.1103/PhysRevC.84.014308

High-resolution study of the ^{9}Be(^{3}He,t)^{9}B reaction up to the ^{9}B triton threshold

C. Scholl,[1,*] Y. Fujita,[2] T. Adachi,[2,3,†] P. von Brentano,[1,‡] H. Fujita,[2] M. Górska,[4] H. Hashimoto,[5] K. Hatanaka,[5] H. Matsubara,[5,6] K. Nakanishi,[6] T. Ohta,[5] Y. Sakemi,[5,7] Y. Shimbara,[8,9] Y. Shimizu,[5] Y. Tameshige,[5] A. Tamii,[5] M. Yosoi,[10,5] and R.G.T. Zegers[8,11]

[1] *Institut für Kernphysik, Universität zu Köln, 50937 Köln, Germany*
[2] *Department of Physics, Osaka University, Toyonaka, Osaka 560-0043, Japan*
[3] *Kernfysisch Versneller Instituut, 9747 AA Groningen, The Netherlands*
[4] *GSI Helmholtzzentrum für Schwerionenforschung GmbH, 64291 Darmstadt, Germany*
[5] *Research Center for Nuclear Physics, Osaka University, Ibaraki, Osaka 567-0047, Japan*
[6] *Center for Nuclear Study, University of Tokyo, RIKEN campus, Wako, Tokyo 351-0198, Japan*
[7] *CYRIC, Tohoku University, Sendai, Japan*
[8] *NSCL, Michigan State University, East Lansing, MI 48824-1321, USA*
[9] *RIKEN Nishina Center, Wako, Tokyo 351-0198, Japan*
[10] *Department of Physics, Kyoto University,Sakyo, Kyoto 606-8502, Japan*
[11] *Department of Physics and Astronomy, Michigan State University, East Lansing, MI 48824, USA*

A high energy-resolution ^{9}Be(^{3}He,t)^{9}B charge-exchange reaction was performed around a scattering angle of 0° and at an intermediate incident energy of 140 MeV/nucleon for the study of precise Gamow-Teller (GT) transition strengths. The energy resolution of 30 keV allowed a precise deconvolution of the spectrum and the determination of angular distributions of cross-sections, excitation energies and decay widths. The GT strength of 10 states has been determined for the first time using the GT strength of the analogous β decays of ^{9}Li and ^{9}C as standards. The large difference between the GT strengths going to the low-lying T=1/2 and the highly excited T=3/2 states is interpreted as a result of their different spatial structures. The obtained GT strength distribution is compared to the results of a (p,n) experiment with lower resolution performed in the 1980s. In particular, the width of the 16.8 MeV, J^π=(5/2$^+$) state has been determined for the first time.

PACS numbers: 21.60.Cs; 25.55.Kr; 27.20.+n;

I. INTRODUCTION

Charge-exchange reactions are an useful tool for determining matrix elements characterizing weak decay processes [1, 2] such as the Gamow-Teller strength. The Gamow-Teller (GT) transition is mediated by a $\sigma\tau$-type operator and is the most common weak process in nuclei. Direct information on the GT transition strength B(GT) is obtained from β-decay studies. Charge-exchange reactions such as (p,n) or (^{3}He,t) are useful tools for the study of B(GT) values [1]. In particular, those performed at angles around 0° and intermediate beam energies (E$\gtrsim$100 MeV/nucleon) were shown to be good probes of GT transition strengths. There is a simple proportionality between the cross sections at linear momentum transfer q=0 of these reactions and the B(GT) values [3]. GT transitions can be accessed by CE reactions without the Q-value limitation of β decay, and B(GT) values can be determined if a standard B(GT) value is known from a β-decay study.

Our interest is in the GT transitions in the A = 9 nuclear system. We performed a high energy resolution ^{9}Be(^{3}He,t)^{9}B experiment, in which precise beam-matching techniques [4–7] were applied. As a result, an improvement in the energy resolution by one order of magnitude (ΔE $\simeq$30 keV) compared to the pioneering (p,n) experiments was realized. However, there is no observed β-decay from ^{9}B to ^{9}Be. Only analogous decays of ^{9}Li and ^{9}C have been observed.

The B(GT) strength and the Fermi strength B(F) are related to the β-decay ft value by the equation

$$B(\mathrm{GT})\,\lambda^2 + B(\mathrm{F}) = \frac{K}{f\mathrm{t}} \qquad (1)$$

where K=6143.6(17)s [8] and λ=g_A/g_V= –1.270(3) [9]. The cross-sections from a charge-exchange experiment at zero degree scattering angle, extrapolated to q=0, allow to determine the corresponding GT strength by using the proportionality [3]

$$\left.\frac{d\sigma}{d\Omega}\right|_{q=0} = \hat{\sigma}_{\mathrm{GT}} B(\mathrm{GT}) \qquad (2)$$

for transitions to Gamow-Teller states, and

$$\left.\frac{d\sigma}{d\Omega}\right|_{q=0} = \hat{\sigma}_{\mathrm{F}} B(\mathrm{F}) + \hat{\sigma}_{\mathrm{GT}} \mathrm{B(GT)} \qquad (3)$$

for transitions to the isobaric analog state (IAS), if both Fermi and Gamow-Teller transitions are allowed. The factors $\hat{\sigma}_{\mathrm{F}}$ and $\hat{\sigma}_{\mathrm{GT}}$ are the *unit cross-sections* for the Fermi- and Gamow-Teller transitions, respectively, and measured in the same units as the experimental differential cross-section. The value of B(F)=(N-Z) is obtained

* e-mail address: scholl@ikp.uni-koeln.de
† currently: Research Center for Electron and Photon Science, Tohoku University, Sendai, Japan
‡ Email address: brentano@ikp.uni-koeln.de

by assuming that the Fermi strength exhausts the full Fermi sum rule [10]. The unit cross-sections can be obtained by calibrating the experimental cross-section with known B(GT) values (i.e. partial lifetimes and branching ratios) from β-decay studies. The close proportionality given in Eq. (2) has been previously examined by comparing the GT transition strengths derived in the (^{3}He,t) measurements with those from mirror β decays for a number of cases in which multiple pairs of analogous GT transitions could be compared, and a good agreement has been found in most cases [11–15]. The absolute values of the Fermi and Gamow-Teller unit cross-sections for the (^{3}He,t) reaction at 140 MeV/nucleon were studied across a wide range of nuclear masses [16]. As a result of these investigations, the empirical formulae

$$\hat{\sigma}_{\rm F} = 72 \cdot A^{-1.06}\ {\rm mb/sr} \tag{4}$$

$$\hat{\sigma}_{\rm GT} = 109 \cdot A^{-0.65}\ {\rm mb/sr} \tag{5}$$

have been shown to be a good approximation of the mass-number dependence of the unit cross-sections. The observed data points have a maximal deviation from the systematics of 5% for $\hat{\sigma}_{\rm GT}$ and 15% for $\hat{\sigma}_{\rm F}$ [16].

The cross-section at linear momentum transfer q=0 and the (experimental) cross-section at zero degree scattering angle are related via kinematic and distortion factors [3]. These factors can be expressed by a factor $F(q,\omega)$ which describes the shape of the cross-section distribution as a function of the momentum transfer q and the energy loss ω=$E_x - Q$ [where Q is the reaction Q-value, Q(^{9}Be(^{3}He,t)^{9}B)= –1086.7(10) keV]. For a fixed reaction, $F(q,\omega)$ only depends on the excitation energy of the considered state and the scattering angle. The factor $F(0,\omega)$ can be calculated in DWBA

$$F(0,\omega) = \frac{\frac{d\sigma}{d\Omega}^{DWBA}(0^\circ,\omega)}{\frac{d\sigma}{d\Omega}^{DWBA}(0^\circ,\omega=0)} \tag{6}$$

and it is quite robust against changes in the DWBA parameters. The factor F goes to unity in the limit of zero momentum transfer and energy loss. It can be used to obtain the cross-section at zero momentum transfer

$$\frac{d\sigma}{d\Omega}\Big|_{q=0} = \frac{d\sigma}{d\Omega}\Big|_{\Theta=0^\circ} \cdot \left(F(0,\omega)\right)^{-1}. \tag{7}$$

The B(GT) value can then be calculated if the unit cross-sections are known [see Eqs. (2) and (3)].

A pioneering ^{9}Be(p,n)^{9}B experiment was performed in the 1980s [17, 18] with an energy resolution of about 400 keV. Since the strength of the GT transition from the β decay that can provide the unit GT cross-section $\hat{\sigma}_{\rm GT}$ was not available at that time, GT strengths could not be deduced. In addition, unlike our experiment with a higher energy resolution of 30 keV, weak and discrete states could not be resolved in the (p,n) experiment. In particular, the state at 14.65 MeV which is needed for the accurate calibration with β-decay data could not be isolated in the (p,n) experiment. The GT strengths could therefore not be determined. A ^{9}Be(^{3}He,t)^{9}B experiment was performed by Akimune *et al.* [19] with an energy resolution of about 150 keV, and found compelling evidence for a state at 3.8 MeV.

We have recently reported preliminary results of our (^{3}He,t) experiment performed with higher energy resolution [7, 20]. The present paper describes the experimental results in detail. We will first report the excitation energies and decay widths of states observed in the spectra and their zero-degree cross-sections deduced from the angular distribution analysis. We will then give the GT strengths obtained from our data using the analogous β-decays of ^{9}Li and ^{9}C for calibration. We will compare our results to the previous (p,n) study. We will also propose an interpretation of the large difference between the values of GT strengths going to the levels with lower excitation energies and to those with higher excitation energies.

II. EXPERIMENT

The experiment was performed at RCNP, Osaka, using a ^{3}He beam accelerated by the K=120 AVF cyclotron and boosted up to 420 MeV (140 MeV/nucleon) by the K=400 ring cyclotron [21]. The beam was guided to the target through the WS beam line [4, 5]. A target of metallic ^{9}Be (1.73 mg/cm^2) was used to study excited states in ^{9}B via the (^{3}He,t) reaction. The outgoing tritons (A/Z=3) were momentum-analyzed by the Grand Raiden spectrometer [22]. In order to achieve a good energy resolution, dispersion matching conditions were realized between the beam line and the spectrometer [4, 23]. The ^{3}He^{++} (A/Z=3/2) beam was dumped into the Faraday cup installed inside the inner bend of the first dipole magnet (D1), which was also used to monitor the beam current. At the focal plane, the particles were traced using multiwire drift chambers (MWDC) for track reconstruction. Two plastic scintillators were used for particle identification and for triggering of the MWDCs [24]. The data was taken at a spectrometer angle of zero degrees. In nearly 5h beamtime with an average beam current of 11.6 nA, 6.4·10^{14} ^{3}He particles were collected in the Faraday cup. The dead time of the focal plane detector and data acquisition system was approximately 6%. The beam integration can have a systematic error, which can influence the absolute value of the differential cross-sections. However, since we use the B(GT) value of the 14.65 MeV state determined from a β-decay study, it has no effect on the derived B(GT) values. The number of beam particles as well as the target thickness cancel when the ratio $\frac{d\sigma}{d\Omega}_{q=0}(E_x) / \frac{d\sigma}{d\Omega}_{q=0}$(14.65 MeV) is calculated [see Eqs. (2) and (8)].

The spectrometer acceptance is about 20 mrad in the horizontal and 40 mrad in the vertical direction, which allowed to study the angular distribution of states from scattering angles of zero up to about $\Theta_{\rm lab}$=2° with one setting. For the analysis of angular distri-

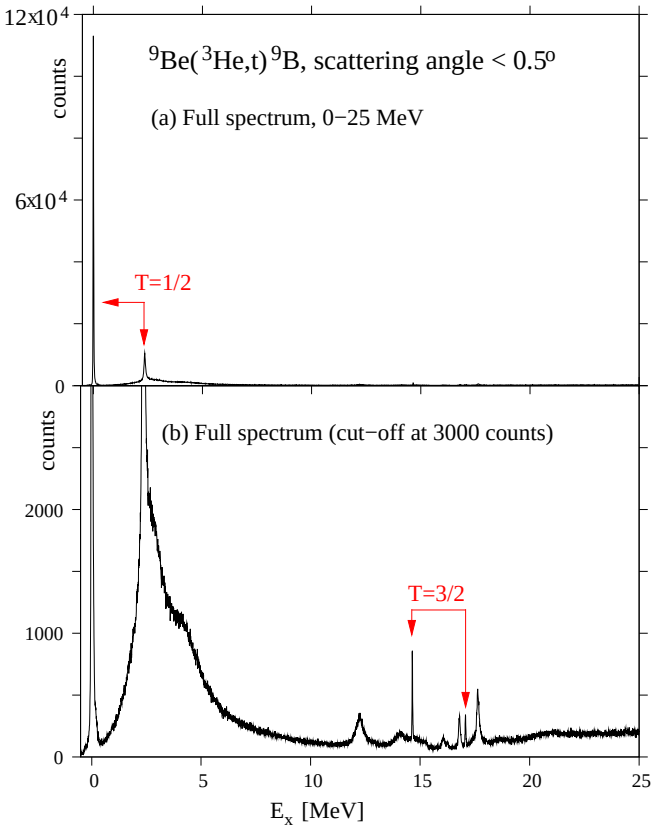

FIG. 1. (Color online) Spectrum of the ^{9}Be(^{3}He,t)^{9}B reaction at 140 MeV/nucleon beam energy and at scattering angles $\Theta \leq 0.5°$.
(a) The full spectrum without any cut-offs. The only prominent peaks are the two T=1/2, J^π=3/2$^-$ (ground state) and J^π=5/2$^-$ (2.4 MeV) states .
(b) The same spectrum with a cut-off at 3000 counts. Weakly excited states at higher excitation energies become visible. The two T=3/2 states at 14.65 MeV (J^π=3/2$^-$) and 17.1 MeV (J^π=1/2$^-$) are marked in the figure.

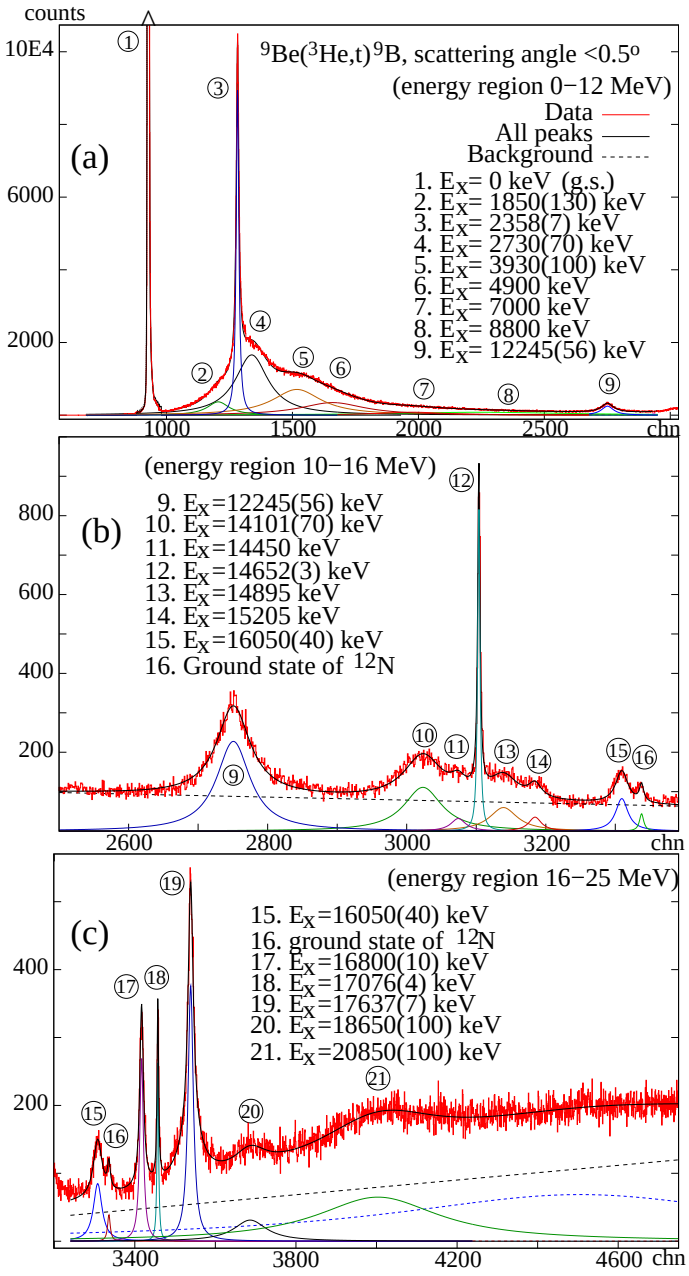

FIG. 2. (Color online) Deconvolution of the energy spectrum of the ^{9}Be(^{3}He,t)^{9}B reaction at 140 MeV/nucleon beam energy, with scattering angle $\Theta \leq 0.5°$. The spectrum has been subdivided in three excitation energy regions for better visibility. In the first spectrum, the ground state peak was cut off (the maximum lies at ≈120,000 counts). The peaks have been deconvoluted using lorentzian shapes folded with a spectrometer-specific reponse function. All peaks have numbered labels corresponding to their excitation energy, which are also used in Table I.

butions, the recorded spectrum was subdivided in four scattering-angle regions using the track information from the MWDCs. The angles (determined in the laboratory frame) were converted into the c.m. frame using CATKIN [25].

The use of the angular distribution data is twofold. It allows to identify the states that are excited via $\Delta\ell$=0 transitions (GT states) and to separate them from the non-GT states. It also allows to extrapolate the cross-section at zero degrees scattering angle, which is needed for the determination of GT strengths using the proportionality given by Eq. (2).

III. ENERGIES AND DECAY WIDTHS

After offline corrections for kinematic effects as well as spectrometer aberrations, energy spectra for different scattering angle regions were obtained. Events within these regions were projected onto the x-axis of the focal plane (measuring the bending radius of the tritons and thus their energy) to obtain these spectra. An energy resolution of about 30 keV was realized. The spectrum for scattering angles between 0° and 0.5° (see Fig. 1) is of main interest for the determination of Gamow-Teller strengths. The spectra at higher angles were used to de-

termine the angular distributions of excited states and identify transitions of $\Delta\ell$=0 (GT) nature, which have a pronounced forward-peaking in their angular distributions. Using several spectra at different scattering angles, the angular distributions were extrapolated to the differential cross section at zero degrees, which is needed to obtain the GT strength.

The excitation energies were calibrated using peaks with well-known excitation energies from the nuclei ^{12,13}N,^{24,26}Al and ^{16,18}F obtained with the same experimental settings.

Some of the excited states in ^{9}B below 10 MeV have large widths and are overlapping, which makes the identification of some individual states rather difficult. All these states below 10 MeV are T=1/2 states. The deconvolution of the spectrum was made on the basis of the evaluation by Tilley *et al.* [26], using the software code SFIT [27]. The deconvolution assumes Lorentzian peak shapes, convoluted with a spectrometer response function (derived from the peak shapes of isolated peaks with no intrinsic width) as shown in Fig. 2. The obtained excitation energies and widths are summarized in Table I and compared to the compiled values.

The first excited state in ^{9}B is deemed to be the analog of the 1.68 MeV, J^{π}=1/2^{+} state of ^{9}Be [26]. The search for this analog state has yielded a wide range of possible energies and widths in previous experimental studies. Since a 1/2^{+} state can only be weakly excited in the (^{3}He,t) reaction at forward angles, this state is buried under the very large bump-like structure arising from the overlapping higher excited states with large widths. The present deconvolution attempt suggests an excitation energy of 1.85(13) MeV for this state [label 2 in Fig. 2(a)], and a decay width of 700^{+270}_{-200} keV. This is broadly in line with previous studies, especially the recent deconvolution analysis of (^{3}He,t) data by Akimune *et al.* [19]. The next state is the strongly excited 5/2^{-} state at 2.358(7) MeV. The excitation energy and the width of this state are in good agreement with the compiled values as shown in Table I.

The spectrum also contains a rather wide and strongly excited state with $\Delta\ell$=0 character at 2.73 MeV [label 4 in Fig. 2(a)]. By using the same (^{3}He,t) reaction at a slightly higher beam energy of 150 MeV/nucleon but with a lower resolution of around 150 keV, this state was also observed in [19]. However, they fixed the position at the excitation energy of 2.788 MeV, which is the value of a state assigned as J^{π}=5/2^{+} [26]. They acknowledged the angular distribution of this state did not follow the expected $\Delta\ell$=1 behaviour for a 5/2^{+} state. The width, however, matched the reported value. The evaluation [26] lists a state at 2.75(30) MeV with J^{π}=1/2^{-} (analog to the 2.78 MeV state in ^{9}Be). This value would explain the observed angular distribution and strong excitation of this state. However, the decay width given in the compilation [3.13(20) MeV] is much larger than the value obtained from our deconvolution [1.0(2) MeV]. The width of $810\pm^{340}_{310}$ keV obtained in [19] is consistent with our value of 1.0(2) MeV.

Akimune *et al.* found compelling evidence for a state at E_x=3.8 MeV [19]. We also clearly see this state [label 5 in Fig. 2(a)] in the present experiment. The angular distribution also supports a $\Delta\ell$=0 character, and the obtained decay width also agrees with the value obtained in [19].

The states listed at 4.8 MeV and 7.0 MeV in [26] are not strongly excited and also do not exhibit a $\Delta\ell$=0 character in their angular distributions. Their excitation energies have been kept fixed at 4.9 and 7.0 MeV for the deconvolution [labels 6 and 7 in Fig. 2(a)]. Although the presence of further strongly excited states in the spectrum can be ruled out, there is some evidence pointing to the presence of one (or more) state(s) with a large decay width at E_x $\simeq$8 MeV excitation energy [there is actually a (5/2^{-}) state listed at 7.94 MeV in ^{9}Be [26]]. It is however very difficult to give an exact position or width for this hypothetical state because of the weak excitation and large ambiguity in the fitting procedure. A good fit was obtained assuming E_x $\approx$8.8 MeV and Γ $\approx$6 MeV.

Peaks that are more easy to deconvolute appear in the spectrum starting with the E_x=12.245(56) MeV, 5/2^{-} state [label 9 in Fig. 2(b)]. The observed excitation energy of this state agrees well with the compiled value, but we found a somewhat smaller decay width of 376(20) keV ($\Gamma^{(NDS)}$=450(20) keV).

The evaluation [26] lists three states between E_x=14 and 15 MeV. As can be seen in Fig. 2(b), a bump-like structure consisting of five peaks exists in the spectrum between 13.8 and 15.3 MeV. Among them, the well-separated 14101^{+50}_{-90} keV state [label 10 in Fig. 2(b), energy and width agree with the evaluated values] shows a $\Delta\ell$=0 angular distribution. This gives the possible spin/parity values J^{π}=(1/2, 3/2, 5/2)$^{-}$). A very sharp state is observed at 14.65 MeV. This state is the T=3/2 analog state of the ^{9}C ground state with J^{π}=3/2^{-}. A detailed discussion of this state is given later.

The evaluation [26] lists a J^{π}=(5/2)$^{-}$ state at E_x=14.70(18) MeV with Γ=1.35(20) MeV, a very broad state at an energy degenerate with the T=3/2 peak at 14.65 MeV. However, the deconvolution of the spectrum cannot be achieved in a satisfactory way assuming the existence of this broad state. Especially the sharp drop of the spectrum at around 15.3 MeV rules out a significant strength with large decay width. Therefore our deconvolution was performed assuming three states [labels 11, 13 and 14 in Fig. 2(b)]. The best fit places these states at E_x=14.45, 14.90 and 15.2 MeV, with decay widths of 175, 330 and 150 keV, respectively. The angular distribution of the whole "bump" shows no significant $\Delta\ell$ $\geq$1 contribution, so that it can be assumed that the whole structure could have GT nature. However, since a decomposition in several smaller states is required in order to reproduce the total structure, we did not attempt to extract a GT strength for the three states derived from the deconvolution. Rather, we will give an upper limit

label in Fig. 2	$\Delta\ell$	$E_x^{(EXP)}$ [keV]	$E_x^{(NDS)}$ [keV]	J^π (NDS)	$\Gamma_{c.m.}^{(EXP)}$ [keV]	$\Gamma_{c.m.}^{(NDS)}$ [keV]
①	0	0.0(3)	g.s.	$\frac{3}{2}^-$	$0.0^{+0.5}$	0.54(21)
②	≥1	1850(130)	≈1600[a]		700^{+270}_{-200}	≈700
			1800^{+220}_{-160} [19]			600^{+300}_{-270} [19]
③	0	2358(7)	2361(5)	$\frac{5}{2}^-$	84(7)	81(5)
④	0	2730(70)	2750(300)[b]	$\frac{1}{2}^-$	1000(200)	3130(200)
			2788(30)[b]	$\frac{5}{2}^+$		550(40)
						810^{+340}_{-310} [19]
⑤	0	3930(100)	3820^{+230}_{-220} [19]		1570(250)	1330^{+620}_{-360} [19]
⑥	≥1	4900[c]	4800(100)		2000(500)	1200(200)
⑦	≥1	7000[c]	6985(50)	$\frac{7}{2}^-$	2190[c]	2180(150)
⑧	≥1	8800[d]				≈ 6000
⑨	0	12245(56)	12190(40)	$\frac{5}{2}^-$	376(20)	450(20)
⑩	0	14101^{+50}_{-90}	14010(70)	$\pi = -$	454(35)	390(110)
⑪	0[e]	14450[e]			175	
⑫	0	14652(3)	14655(3)	$\frac{3}{2}^-$, $T=\frac{3}{2}$	$0.0^{+7.0}$	0.395(42)
⑬	0[e]	14895[e]	14700(180)	$(\frac{5}{2}^-)$	330	1350(200)
⑭	0[e]	15205[e]	15290(40)		150	
⑮	0	16050(40)	16024(25)		155(20)	180(16)
⑰	≥1	16800(10)	16710(100)	$(\frac{5}{2}^+)$	81(5)	
⑱	0	17076(4)	17076(4)	$\frac{1}{2}^-$, $T=\frac{3}{2}$	22.5(35)	22(5)
⑲	≥1	17637(7)	17638(10)		102(18)	71(8)
			17540(100)[f]	$(\frac{7}{2}^+)$ [28]		
⑳	≥1	18650(100)	18600(300)		680(140)	1000
㉑	≥1	20850(100)	20700(500)		2560(220)	1600(300)

TABLE I. Summary of the spectrum deconvolution. The observables presented in columns indicated by a (NDS) superscript denote values from the evaluation by Tilley *et al.* [26], unless another citation is given. All states are identified by the labels in Fig. 2 which are given in the first column.
[a] A wide range of excitation energies and widths have been given from searches for the analog of the 1.68 MeV $1/2^+$ state of ^{9}Be [26]. The values obtained by Akimune *et al.* [19] for the excitation energy and width of this state are in good agreement with our values.
[b] A $5/2^+$ and a $1/2^-$ state have been reported in this energy range [26]. See discussion in text.
[c] This value has been kept fixed for the deconvolution.
[d] This state is not present in the previous evaluations. The deconvolution of the spectrum supports the presence of an additional very broad peak within this energy range.
[e] The bump-like structure between 13.8 and 15.3 MeV was deconvoluted based on the clearly separated peaks at 14.1 MeV and 14.65 MeV. It was found that three states are needed to correctly reproduce the observed spectrum (see discussion in text). They are given with the fitted positions and width, without errors. The state at the edge of the bump, at E_x=15.2 MeV might correspond to the 15.3 MeV state in the compilation. The angular distribution of the whole structure has $\Delta\ell$=0 character.
[f] level from unpublished work on ^{9}Be(p,n) [17, 18], which might not be distinct from the 17.637(10) MeV level [26]. The angular distribution of the observed 17.637(7) MeV peak does not have $\Delta\ell$=0 character.

for the GT strength that can be derived from the zero degree cross-section of the whole structure.

Near the contaminant ^{12}N ground state peak, a well-separated state was observed at 16050(40) keV [label 15 in Fig. 2(c)], which agrees well with the compiled value of 16024(25) keV (the obtained width also agrees, see Table I). This state does not have a spin/parity assignment. Since the angular distribution supports a $\Delta\ell$=0 character, it can have J^π=$1/2^-$, $3/2^-$, $5/2^-$.

The second T=3/2 state of ^{9}B at 17.1 MeV (the analog of the first $1/2^-$ state in ^{9}Li and ^{9}C) is seen as a narrow peak in the (^{3}He,t) spectrum [label 18 in Fig. 2(c)]. Its excitation energy is known with good accuracy (±4 keV) from its γ decay to the ground state.

Some 300 keV lower, we observed a rather sharp state at E_x=16.8 MeV [label 17 in Fig. 2(c)]. A state at 16.71(10) MeV is suggested [26] from the unpublished work on the ^{9}Be(p,n) reaction [17, 18]. Dixit *et al.* [28] observed its analog state in ^{9}Be at 16.671(8) MeV, which is assigned J^π=$5/2^+$. This assignment is supported by the observed angular distribution of this state in the (^{3}He,t) reaction which exhibits a $\Delta\ell \geq 1$ character. We believe the energy value E_x=16.800(10) MeV is more precise than the compiled value, since the state can be well

separated from the T=3/2 state at 17.1 MeV owing to the high energy resolution in our experiment. We derive a new value of 81(5) keV for the decay width of this state in the present study. The mirror ($5/2^+$) state in ^{9}Be at E_x=16.671(8) MeV has Γ=41(4) keV.

At 17.637(7) MeV, a peak with Γ=102(18) keV was observed [label 19 in Fig. 2(c)]. There are two levels listed in the compilation which correspond to this energy, and it might be [26] that both levels are not distinct. One state at 17.54(10) MeV is given with J^π=($7/2^+$) from unpublished ^{9}Be(p,n) work [17, 18] and is thought to be the analog of the 17.49 MeV, $7/2^+$ state in ^{9}Be observed by Dixit *et al.* [28]. The other compiled state lies at 17.638(10) MeV with a decay width of 71(8) keV. The energy assigned in the present study [E_x=17.637(7) MeV] agrees well with the second value. However the width is smaller than our value [Γ=102(18) keV]. The evaluated decay width is the average of 71(8) keV obtained from a ^{7}Be(d,n) experiment and 70(20) keV from a ^{6}Li(^{3}He,α) study [26]. The angular distribution of this peak has a $\Delta\ell \geq 1$ character.

Two more levels are compiled above 18 MeV excitation energy in ^{9}B. Both are broad and located near to the neutron and triton separation energies. We observe the first level [given at E_x=18.6(3) MeV with Γ=1 MeV in [26]] at 18.65(10) MeV with a width of 680(140) keV [label 20 in Fig. 2(c)]. The ^{8}B+n separation threshold lies at 18.577 MeV. The highest compiled state is at E_x=20.7(5) MeV with Γ=1.6(3) MeV [26]. We observe this level at 20.85(10) MeV with a larger width of Γ=2.56(22) MeV [label 21 in Fig. 2(c)]. The ^{6}Be+t separation threshold lies at 20.909 MeV.

IV. GAMOW-TELLER STRENGTHS

Gamow-Teller strengths can be extracted from the obtained spectra using the proportionality between the differential cross-sections at momentum transfer zero and the B(GT) strengths. For this purpose, we extrapolated the cross-sections at zero degrees scattering angle using the experimental angular distributions. The cross-section at momentum transfer zero can then be calculated by using the kinematic and distortion factors [3] obtained from distorted-wave Born approximation (DWBA) calculations.

The differential cross-sections were calculated using

$$\frac{d\sigma(\Theta_i)}{d\Omega_{c.m.}} = \frac{1}{f^2\Omega_i} \cdot \frac{N_{\rm triton}(\Theta_i)}{n_{\rm target} \cdot N_{^3{\rm He}}} \tag{8}$$

$$= \frac{1}{(1.372)^2(0.239246 \cdot 10^{-3}\ sr)(6.3565 \cdot 10^{14})} \times$$
$$\times \frac{9.012 \cdot 10^3\ {\rm g \cdot mol^{-1}} \cdot 10^{27}\ {\rm mb \cdot cm^{-2}}}{1.0 \cdot 1.73\ {\rm g \cdot cm^{-2}} \cdot 6.022 \cdot 10^{23}\ {\rm mol^{-1}}} \cdot \frac{N_{\rm triton}(\Theta_i)}{\Omega_i/\Omega_1}$$
$$= (3.02176 \cdot 10^{-5}\ mb/sr) \cdot \frac{N_{\rm triton}(\Theta_i)}{\Omega_i/\Omega_1}. \tag{9}$$

Here, $N_{\rm triton}(\Theta_i)$ is the number of tritons observed in the focal plane at angle Θ_i (i.e. in the corresponding scattering angle bin Ω_i, with $\Omega_1 \approx 0.24 \cdot 10^{-3}$sr) that can be attributed to the charge-exchange reaction for a given number of incident ^{3}He particles ($N_{^3{\rm He}}$=6.3565·10^{14}) on the target. The value $N_{\rm triton}(\Theta_i)$ has to be adjusted for the efficiency of the detection system, which is around 90%. The value $n_{\rm target}$ gives the number of target nuclei per unit area (calculated using $N_A = 6.022 \cdot 10^{23}{\rm mol}^{-1}$, a target enrichment of 100%, the molar mass of ^{9}Be (9.012 g $\cdot$ mol^{-1}) and the target thickness of 1.73 mg/cm^2). The solid angle in the laboratory frame (Ω_i) is transformed into the solid angle $\Omega_{c.m.}$ in the center of mass frame via the factor f which connects both frames. The factor f can be calculated relativistically and we obtain f = 1.372 for the beryllium target. The average angle Θ_i (laboratory frame) used to represent each angular bin was calculated in a way such that it would halve the surface of the corresponding area in the plane spanned by the horizontal and vertical scattering angles.

It should be noted that $N_{^3{\rm He}}$ and $n_{\rm target}$ can be subject to systematic errors due to the current integration and the determination of target thickness. However, since we use the unit cross-section derived from β-decay measurements, these errors will not be taken into account when analyzing the angular distributions and determining the B(GT) values. Systematic variations in $N_{^3{\rm He}}$ and $n_{\rm target}$ affect all cross-sections in the same way and thus have no influence on the B(GT) values after calibration. The only error that is considered for the angular distributions is the statistical error of $N_{\rm triton}$ arising from the deconvolution. The uncertainty of the standard B(GT) value from β-decay that is used for calibration of the unit cross-section $\hat{\sigma}_{GT}$ will also be taken into account when determining the B(GT) values.

The obtained angular distributions were compared to those calculated in DWBA using the program FOLD [29]. This code uses the Love-Franey nucleon-nucleon interaction [30, 31], double-folded over the projectile-ejectile and target-residue transition densities. A short-range approximation [30] is used for the exchange terms in the potential. Radial wave functions were calculated using the Woods-Saxon potential (parameters from [32]) with the code WSAW, a part of the FOLD package. For the outgoing triton channel, by following the arguments given by Van der Werf *et al.* [33], the well depths were multiplied by a factor of 0.85 without changing the geometrical parameters of the optical potential (radii and diffuseness). The parameters used are listed in Table II.

The 0° cross-sections of observed GT states are summarized in Table III. These cross-sections can then be used to calculate the cross-section at momentum transfer q=0 by dividing by the calculated factor $F(0,\omega)$ [see Eqs. (6) and (7)]. The cross section at 0° scattering angle and zero momentum transfer can then be used to determine the Gamow-Teller strength of the corresponding state. The individual angular distributions $\frac{d\sigma}{d\Omega}(\Theta_{c.m.})$ of GT states, together with the fitted DWBA curves, are

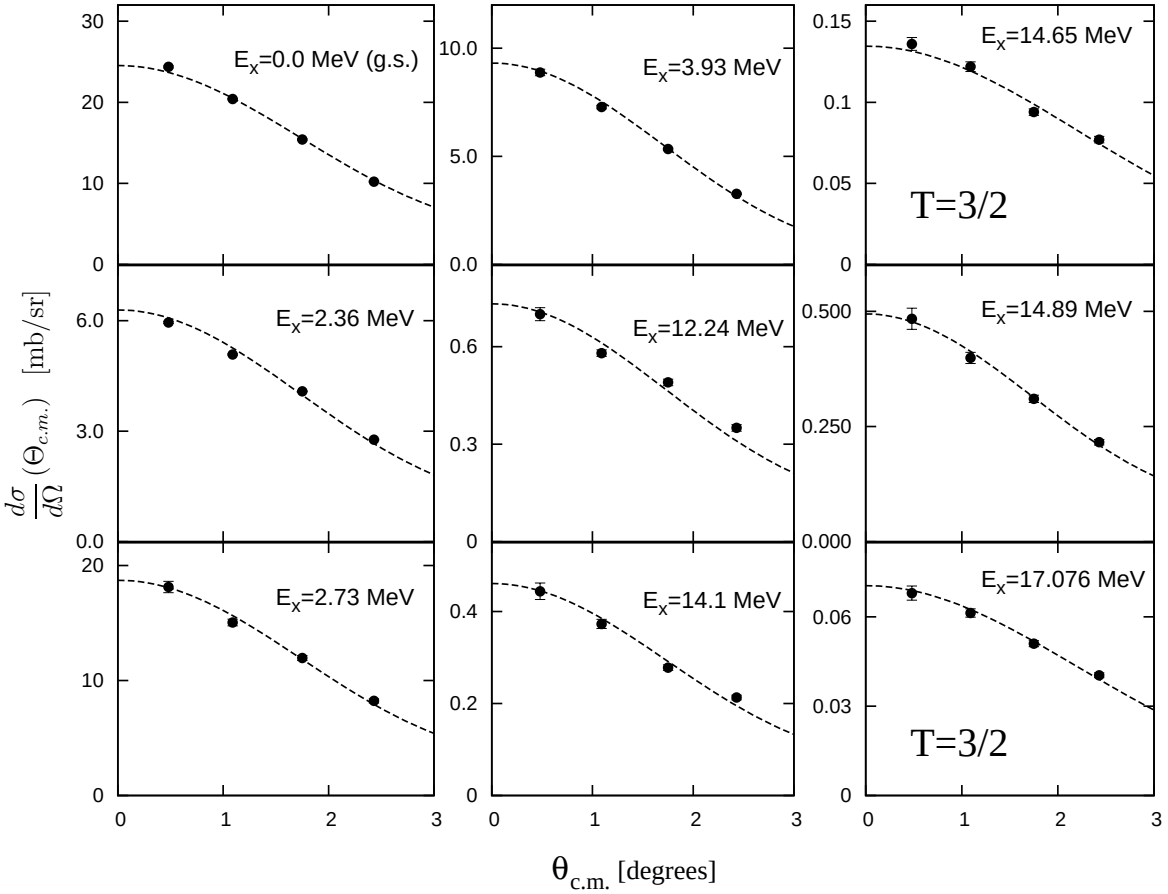

FIG. 3. Angular distribution of cross-sections around zero degree scattering angle of states excited with $\Delta\ell$=0. The line is the angular distribution calculated in DWBA, multiplied for each state by a single scaling factor, which is used to extrapolate the cross section at zero degree scattering angle from the experimental cross-sections. For the T=3/2 states, the DWBA parameters were changed to obtain a good fit to the experimental data. The differential cross-sections were calculated using eq. (8). As mentioned in the text, the errorbars only include the statistical errors arising from the deconvolution of the spectrum.

shown in Fig. 3. The errorbars show only the statistical error arising from the deconvolution of the spectrum, and do not account for systematic errors (mainly the beam intensity and target thickness) which would have the effect of scaling the entire set of derived cross-sections by a single scaling factor. The same DWBA calculation parameters were used to calculate the angular distributions of all T=1/2 states. For the two T=3/2 states, the optical DWBA parameters were adjusted to obtain a good fit of the experimental data (see Fig. 3). The radii and diffuseness were decreased by 15%, and the potential depths by 20% (See Table II).

	$V_{\rm R}$ [MeV]	$r_{\rm R}$ [fm]	$a_{\rm R}$ [fm]	$V_{\rm I}$ [MeV]	$r_{\rm I}$ [fm]	$a_{\rm I}$ [fm]
T=1/2	-140	1.10	0.78	-70	0.60	0.61
T=3/2	-112	0.94	0.66	-56	0.51	0.52

TABLE II. Parameters used for the DWBA calculation of angular distributions. Only the values for the incident channel are given, the values for the outgoing triton channel are obtained by multiplying the well depths by a factor 0.85 (see text).

By using the extrapolated cross-sections at q=0 and the proportionality given by Eqs. (2) and (3), the B(GT) strengths can be determined. Equations (4) and (5) give unit cross-sections $\hat{\sigma}_F$=7.01 mb/sr and $\hat{\sigma}_{GT}$=26.13 mb/sr for A=9 ($R^2_{(^3{\rm He,t})}=\hat{\sigma}_{GT}/\hat{\sigma}_F$=3.73 for A=9). However, since the ground state of ^{9}B is unbound, there is no known β decay from ^{9}B that can be used for calibration purposes.

The Gamow-Teller unit cross-section can, however, be obtained by using the B(GT) values of the analog β decays from ^{9}Li and ^{9}C (see Fig. 4). Studies of the ^{9}C β^+ decay were carried out by Buchmann *et al.* [34], Bergmann *et al.* [35] and Mikolas *et al.* [36], and studies of the ^{9}Li β^- decay by Nyman *et al.* [37] and Prezado *et al.* [38].

$$B(GT;^9\,{\rm C(g.s.)} \rightarrow ^9\,{\rm B(g.s.)}) = 0.0183(5) \quad (10)$$

$$B(GT;^9\,{\rm Li(g.s.)} \rightarrow ^9\,{\rm Be(g.s.)}) = 0.0181(6) \quad (11)$$

These values were derived from those compiled by Tilley *et al.* [26]. Analogous Gamow-Teller strength was also

label in Fig. 2	E_x [keV]	J^π	$F(0,\omega)$	$\frac{d\sigma}{d\Omega}$ (0°) [mb/sr]	$\frac{d\sigma}{d\Omega}$ ($q=0$) [mb/sr]	B(GT) from (^{3}He,t)
①	0.0(3)	$\frac{3}{2}^-$	0.997	24.53(6)	24.61(6)	0.66(18)[a]
③	2358(7)	$\frac{5}{2}^-$	0.985	6.29(1)	6.38(1)	0.241(8)
④	2730(70)	$\frac{1}{2}^-$	0.983	18.71(20)	19.0(2)	0.718(24)
⑤	3930(100)	$(\frac{1}{2},\frac{3}{2},\frac{5}{2})^-$	0.974	9.31(5)	9.56(5)	0.360(12)
⑨	12245(56)	$\frac{5}{2}^-$	0.875	0.732(9)	0.836(10)	0.0315(11)
⑩	14101^{+50}_{-90}	$(\frac{1}{2},\frac{3}{2},\frac{5}{2})^-$	0.845	0.461(6)	0.545(7)	0.0205(7)
⑫	14652(3)	$\frac{3}{2}^-$, T=$\frac{3}{2}$	0.836	0.135(1)	0.161(2)	0.0061(2)
⑪⑬⑭	14895	$(\frac{5}{2}^-)$	0.832	0.494(7)	0.594(9)	≤0.0224(8)[b]
⑮	16050(40)	$(\frac{1}{2},\frac{3}{2},\frac{5}{2})^-$	0.812	0.065(1)	0.0806(18)	0.00304(12)
⑱	17076(4)	$\frac{1}{2}^-$, T=$\frac{3}{2}$	0.793	0.0705(8)	0.0889(1)	0.00335(11)
					Σ	2.07(18)

TABLE III. Experimentally derived B(GT) values for ^{9}Be(g.s.)→^{9}B(E_x) obtained by using the B(GT) values from the studies of the β decay of the nuclei ^{9}C and ^{9}Li. The errors are the statistical uncertainties only (arising from the fitting of the triton spectra) and do not include possible systematic errors arising from the beam current integration or target thickness determination. The factor $F(0^\circ,\omega)$ relates the 0° cross-sectionto the cross-section at q=0 [see eq. (7)]. The energy loss ω is defined as ω=$E_x - Q$ (Q is the reaction Q-value).
[a] Obtained using R^2 from systematics (see text), leading to a larger error for this value. See Eq. (14).
[b] Upper limit B(GT) value for the bump-like structure (see text). This value was included in the total sum of B(GT) strength.

studied in the experimental work of Dangtip *et al.* [39] using the ^{9}Be(n,p)^{9}Li reaction.

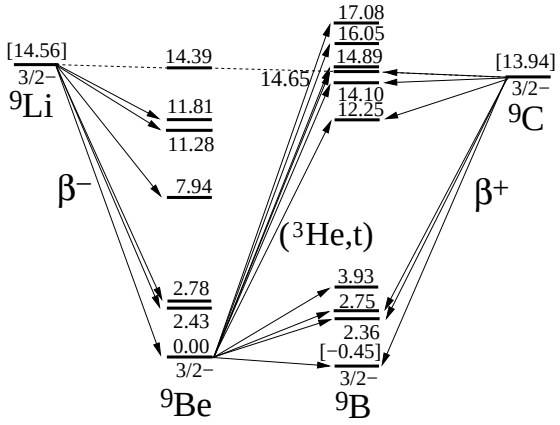

FIG. 4. The A=9 isobar diagram. The arrows show the start and end point as well as the direction of the transitions ^{9}Li(β^-)^{9}Be, ^{9}Be(^{3}He,t)^{9}B and ^{9}C(β^+)^{9}B. Adapted from [26]. The diagrams for individual isobars are shifted vertically to eliminate the neutron-proton mass difference and the Coulomb energy. The energies in square brackets represent the approximate nuclear energy $E_{\rm N}$=$M(Z,A) - Z\,M(H) - N\,M(n) - E_{\rm C}$, minus the corresponding quantity for ^{9}Be.

Large asymmetries in the B(GT) values have been observed in the A=9 system for decays from ^{9}Li and ^{9}C to excited states (e.g. the $5/2^-$ states around 12 MeV in ^{9}Be and ^{9}B [38]). However, the decays to the ground states of ^{9}Be and ^{9}B exhibit no asymmetry. The B(GT) value in the direction of the (^{3}He,t) charge-exchange reaction can be derived by adjusting the Clebsch-Gordan coefficients [40] for the different spin and isospin values (J^π,T,T_z) of the initial and final states [1]. Using the B(GT) values from the ^{9}C β^+ decay [Eq. (10)], we obtain the B(GT) value for the ^{9}Be(g.s.)→^{9}B(E_x=14.655 MeV) transition

$$B(\mathrm{GT};{}^9\mathrm{Be}_{(\frac{3}{2}^-,\frac{1}{2},+\frac{1}{2})} \rightarrow {}^9\mathrm{B}_{(\frac{3}{2}^-,\frac{3}{2},-\frac{1}{2})}) = \frac{1}{3}\cdot 0.0183(5) = 0.0061(2).$$

where the subscripts are the values of J^π,T and T_z, respectively. In the same way, by using the value from the ^{9}Li β^- decay [Eq. (11)], B(GT)=0.0060(2) is obtained. In the present study, we shall use the value B(GT,^{9}Be$_{g.s.}$ →^{9}B$_{14.65\ \mathrm{MeV}}$)=0.00607(18) as the calibration value for the Gamow-Teller unit cross-section. The value is given as B(GT)=0.0061(2) in Table III.

Using this transition to calibrate the GT unit cross-section has the disadvantage that the Q-value for this transition is rather large (∼16 MeV) which means that the momentum transfer in the (^{3}He,t) reaction is relatively large. The value of the cross-section at zero momentum transfer has to be extrapolated using the factor F(0,ω) calculated in DWBA. This is, however, the only practicable way since there is no known ground state β decay of ^{9}B.

Using F(0,ω=15.74 MeV)=0.836 and the zero-degrees cross-section extrapolated from the angular distribution data [0.135(1) mb/sr], one obtains

$$\left.\frac{d\sigma}{d\Omega}\right|_{q=0}(E_x = 14.655 MeV) = 0.161(2)\ \mathrm{mb/sr}. \quad (12)$$

[1] The B(GT) strength is related to the reduced matrix element M_{GT} via $B(\mathrm{GT})=\frac{\langle T_i T_{zi}\Delta T\Delta T_z|T_f T_{zf}\rangle^2}{2(2J_i+1)(2T_f+1)} M_{GT}^2$

Using this value and B(GT)=0.00607(18), as shown above, the obtained GT unit cross-section is 26.5(8) mb/sr, which is consistent with the value of 26.13 mb/sr obtained from the systematics [Eq. (5)]. The errors do not include the systematic errors stemming from the beam normalization and the target thickness. The fact that the obtained experimental unit GT cross-section is consistent with the mass number systematics is important. The B(GT) value used for the calibration is very small, and it has been observed in several cases that for small B(GT) values the proportionality does not always hold (*e.g.* in ^{34}Cl [15] or ^{58}Ni [41]). The reason is thought to be that the contribution of the tensor-τ part of the effective projectile-target interaction can be large in these cases [14–16, 41]. Since the systematic study of Zegers *et al.* [16] excludes these effects, the agreement of the GT unit cross-section derived from the empirical formula [Eq. (5)] and the experimental GT unit cross-section indicates that we do not suffer much from this effect. We can thus rely on the proportionality and the deduced GT unit cross-section as a calibration standard. It should however be noted that the trendline for the unit cross-section in [16] was only determined down to A=12 and that we use an extrapolation to a lower mass number. This can be a further source of uncertainty.

Using the GT to F unit cross-section ratio $R^2=\hat{\sigma}_{\rm GT}/\hat{\sigma}_F$=3.7(6) obtained from the systematics[2], the Fermi unit cross-section can be calculated as

$$\hat{\sigma}_{\rm F} = \frac{\hat{\sigma}_{\rm GT}}{R^2} = \frac{26.5(8)}{3.7(6)} = 7(1)\ \text{mb/sr}. \qquad (13)$$

This Fermi unit cross-section can be used to extract the B(GT) strength in the ground state transition (^{9}Be$_{g.s.}$ $\rightarrow^9$B$_{g.s.}$). Following Eq. (3), we obtain [assuming that the total Fermi strength of B(F)=$(N-Z)$=1 is contained in the transition to the IAS]

$$\left.\frac{d\sigma}{d\Omega}\right|_{\substack{E_x=0\\ q=0}} = \hat{\sigma}_{\rm F}\cdot 1 + \hat{\sigma}_{\rm GT}\ \cdot\ B(\mathrm{GT};{}^9\mathrm{Be_{g.s.}}\rightarrow{}^9\mathrm{B_{g.s.}})$$

$$\Leftrightarrow B(\mathrm{GT};{}^9\mathrm{Be_{g.s.}}\rightarrow{}^9\mathrm{B_{g.s.}}) = \frac{1}{\hat{\sigma}_{\rm GT}}\left(\left.\frac{d\sigma}{d\Omega}\right|_{\substack{E_x=0\\ q=0}} - \hat{\sigma}_{\rm F}\right)$$
$$= 0.66(18) \qquad (14)$$

Due to the uncertainty of the unit cross-section systematics, the error given for the B(GT;^{9}Be$_{g.s.}$ $\rightarrow^9$B$_{g.s.}$) value is much larger than the uncertainties of B(GT) strengths of pure GT transitions. All other (pure) B(GT) strengths were obtained by dividing the extrapolated 0°, q=0 cross-sections by the determined $\hat{\sigma}_{\rm GT}$. The results are summarized in Table III and the B(GT) strength distribution is shown in Fig. 5(a).

[2] The error is derived from the error of the systematics indicated in [16] (5% for $\hat{\sigma}_{\rm GT}$ and 15% for $\hat{\sigma}_{\rm F}$)

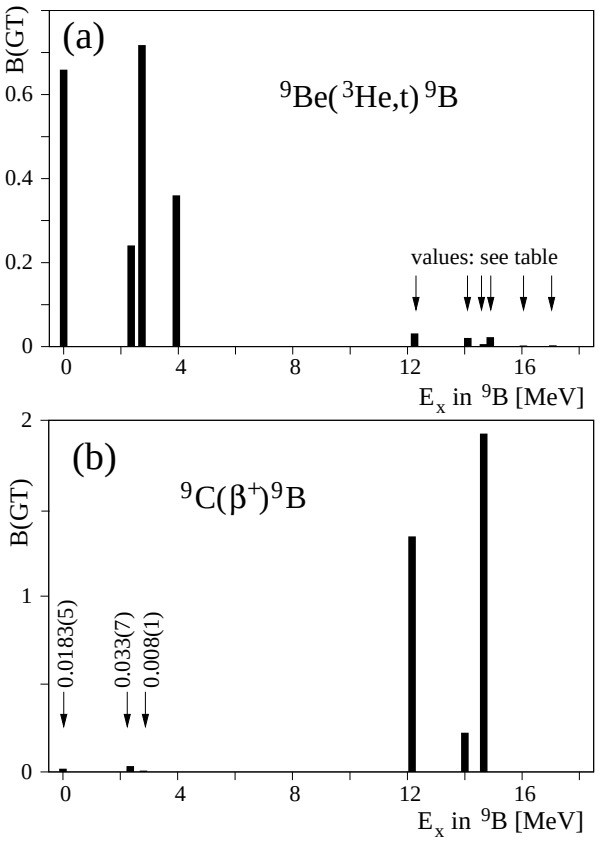

FIG. 5. (a) Distribution of B(GT) strengths obtained from the ^{9}Be(^{3}He,t)^{9}B charge-exchange reaction studied in this work. Transitions to low-lying states in ^{9}B have large GT strength, whereas the transitions to the highly excited states in ^{9}B have very small GT strengths. The B(GT) values of all observed GT transitions, including the weak transition strengths indicated by arrows, are given in Table III.
(b) The same pattern is seen in the "reverse" transition, which shows the distribution of B(GT) strengths obtained from the β^+ decay of ^{9}C (data from [26], [34] and [35]). The ^{9}C β^+ decay exhibits strong GT transitions to the highly excited states in ^{9}B, and weak GT transition strengths to the low-lying states. See the A=9 isobar diagram in Fig. 4 for the energy difference, starting and end points of the respective transitions.

V. COMPARISON WITH (p,n) DATA

The Gamow-Teller strengths can also be determined from the cross-sections measured in the (p,n) reaction [3, 42]. By analyzing the ^{9}Be(p,n)^{9}B reaction at E_p=135 MeV, Pugh obtained differential cross-sections for GT transitions to the excited states in ^{9}B [17, 18]. In order to compare with our (^{3}He,t) results, these cross-sections were converted into B(GT) values. Since the J^π=5/2$^-$, sharp and strong GT state at 2.36 MeV was clearly observed in both the (p,n) and (^{3}He,t) reactions, we used our value B(GT)=0.241(8) as the normalization standard for the conversion.

The 0° cross-sections obtained by Pugh were first modified to q=0 cross-sections by using the F(0,ω) factor

calculated in DWBA. The proton bombarding energy of E_p=135 MeV, and the optical potential parameters Pugh used for the fitting of cross-sections in his experiment (V_R=16.2 MeV, r_R=1.2 fm, a_R=0.66 fm, W_I=11.1 MeV, r_I=1.28 fm and a_I=0.63 fm [17]) were used for the calculation. The normalization to the B(GT) strength of the 2.36 MeV state yields a GT unit cross-section of

$$\hat{\sigma}_{\rm GT}^{(p,n)} = \frac{2.13(4)\ {\rm mb/sr}}{0.241(8)} = 8.85(34)\ {\rm mb/sr} \qquad (15)$$

which agrees well with the systematic trend of the (p,n) GT unit cross-sections [3]. All q=0 cross-sections (except for the ground state) were then divided by $\hat{\sigma}_{GT}^{(p,n)}$ to obtain the corresponding B(GT) strengths. The results are shown in Table IV. The ground state B(GT) value was derived using Eq. (14). The ratio R^2 was taken from the systematics for (p,n) experiments [3], assuming a 10% error:

$$R^2_{(p,n)} = \left(\frac{E_p(MeV)}{55}\right)^2 = 6.0(6)\ . \qquad (16)$$

The B(GT) value for the ground state transition obtained in this way is B(GT,E_x=0) = 0.91(15), which agrees within the errorbars with the value of 0.66(18) obtained from the (^{3}He,t) data.

$E_x^{(p,n)}$ [MeV]	$F(0,\omega)^{(a)}$	$\frac{d\sigma}{d\Omega}^{(p,n)}(0^\circ)$ [mb/sr]	$\frac{d\sigma}{d\Omega}^{(p,n)}(q=0)$ [mb/sr]	$B({\rm GT})^{(p,n)}$ from [17]$^{(b)}$
0	0.995	9.52(4)	9.56(4)	0.91(15)$^{(c)}$
2.36	0.98	2.09(4)	2.13(4)	0.24(1)$^{(b)}$
2.71	0.977	2.83(36)	2.9(4)	0.33(4)
2.75	0.977	9.73(29)	10.0(3)	1.13(5)
4.3	0.962	2.41(6)	2.50(6)	0.28(1)
12.2	0.848	0.230(14)	0.27(2)	0.031(2)
14	0.814	0.0657(22)	0.081(3)	0.0091(5)
14.6	0.802	0.213(25)	0.27(3)	0.030(4)
15.9	0.775	0.0578(59)	0.075(8)	0.0084(9)
16.7	0.759	0.0441(50)	0.058(7)	0.0066(8)
			Σ	2.98(16)

TABLE IV. B(GT) values for ^{9}Be(g.s.)$\rightarrow^9$B(E_x) deduced from the cross-section data of the ^{9}Be(p,n) experiment [17, 18]. The B(GT) values of strong and well-separated GT states agree with the (^{3}He,t) results, while weaker states and states that are near to other $\Delta\ell \geq$1 states that cannot be resolved in the (p,n) reaction result in much higher B(GT) values (see text).

$^{(a)}$ The F factor was determined by DWBA calculation, using the parameters given in [17].

$^{(b)}$ The B(GT) values were derived from the zero-degree cross-sections from [17], using the 2.36 MeV state [B(GT)=0.241(8)] as a standard (see text).

$^{(c)}$ The ground state B(GT) was calculated using Eq. (14) and using the R^2 value obtained from (p,n) systematics [3].

The B(GT) values obtained for the strongly excited states that could be resolved in the (p,n) reaction (E_x=0.0, 2.36 and 12.2 MeV) agree with the (^{3}He,t) results. In the case of the 2.36 MeV state, the agreement is enforced due to the normalization. Especially the B(GT) value for the 12.2 MeV state [0.031(2)], which is the strongest among the higher excited states and is also well separated from other states, agrees with the (^{3}He,t) value [0.0315(11)], which shows that the proportionality holds well in both reactions.

The sharp T=3/2 state at 14.65 MeV [which was used for the calibration of the (^{3}He,t) data] is not present as a sharp state in the (p,n) spectrum and could not be well separated from the "bump" structure (see section III) between 14 and 15 MeV. A calibration using the cross-section of this state is thus not possible. It should be noted that the main difference in the results from the (p,n) and the (^{3}He,t) reactions is a result of the different energy resolutions. The 14 MeV state is also not clearly separated. The whole strength in the 14–15 MeV region is in better agreement although there are more states observed in the (^{3}He,t) spectrum. From the (p,n) data, we obtain ΣB(GT)=0.0091(5) + 0.030(4) = 0.039(4) and from the (^{3}He,t) data ΣB(GT)=0.049(1) (sum of the strengths of the 14.1 MeV state, the 14.6 MeV state and the 14.9 MeV state) which is in better agreement than the individual B(GT) strengths. The good agreement is an indication that this region contains little or no $\Delta\ell \geq$1 strength.

This separation problem also arises for the states observed at 15.9 MeV and 16.7 MeV in the (p,n) reaction [17, 18]. Both states are near to the 16.8 MeV state and the 17.6 MeV state. In our analysis, both of these states have $\Delta\ell \geq$1 character and significant cross-sections. Therefore, the B(GT) values of both states being larger by a factor of two in the (p,n) results is not suprising.

The total B(GT) strengthis more than 40% larger in the (p,n) result (ΣB(GT)=2.98) compared to the (^{3}He,t) result (ΣB(GT)=2.07). The difference is mainly caused by the treatment of the broad states in the region E_x=2–4 MeV. Pugh assumes a 2.71 MeV state and a 2.75 MeV state in this region [17], which yield a total B(GT) value of 1.46. On the other hand, we only see one $\Delta\ell$=0 state at 2.73 MeV in the (^{3}He,t) reaction, which has a B(GT) value of only 0.718(24). Looking at the spectrum decomposition of the (p,n) data in [17], the 2.75 MeV state is shown as a very broad peak with a width of 3.1 MeV. In addition, an asymmetric shape had to be introduced to obtain a good agreement with the measured spectrum. Due to the large width and large strength required for this state in the (p,n) spectrum to fit the low-energy "bump" with only two states, the higher energy tail of this state stretches up to the 10 MeV region. On the other hand, from our measurements with higher resolution, we know that the low-energy region of the charge-exchange reaction is made up of several peaks of both $\Delta\ell$=0 and $\Delta\ell \geq$1 nature (See Table I). It is therefore understandable that the GT strength obtained from the (p,n) data is far too large in the low-lying region. The

B(GT) values for the other weak or overlapping states could not be determined from the (p,n) reaction in a reliable way because they are often masked by $\Delta\ell \geq 1$ strength. The (^{3}He,t) reaction, however, can determine more reliable cross-sections and thus B(GT) values for these states since the energy resolution is better by about one order of magnitude.

VI. INTERPRETATION OF RESULTS

High-resolution studies of B(GT) strength in light nuclei are an important testing ground for theoretical nuclear structure calculations, as has been shown *e.g.* for the nucleus ^{11}C [43]. The B(GT) transition strengths are an important observable that state-of-the-art nuclear structure calculations like *ab initio* calculations [no core shell model (NCSM)] or cluster calculations [antisymmetrized molecular dynamics (AMD) or fermionic molecular dynamics (FMD)] should reproduce.

The B(GT) strengths also give insight into the nuclear structure, as can be illustrated here for the ^{9}B case. An immediately obvious feature of the B(GT) strength distribution in ^{9}B (Fig. 5) is that the B(GT) strengths above 14 MeV excitation energy are two orders of magnitude smaller than the B(GT) strengths of the low-lying T=1/2 states with E_x=0–4 MeV.

To understand this, it should be reminded that the GT transition is caused by the action of the $\sigma\tau$ single particle operator, which by its simple form cannot change the spatial shape of the nucleus. The B(GT) strengths to the higher excited energies lying in the excitation energy range of the ground states of the T$_z$=±3/2 nuclei ^{9}Li and ^{9}C are strongly suppressed. This suggests that these states have a different spatial structure than the ground states of ^{9}Be and ^{9}B (the 14.65 MeV state in ^{9}B is the IAS of the ground states of ^{9}Li and ^{9}C). A similar pattern can be observed in the β decays of these T$_z$=±3/2 nuclei to the T$_z$=±1/2 nuclei ^{9}Be and ^{9}B (see Fig. 5). As mentioned, the β^+ decay of ^{9}C to ^{9}B [34, 35, 38] and the β^- decay of ^{9}Li to ^{9}Be [37] have been measured with high precision. These measurements show that the transitions from the ground states of these nuclei to the ground states of ^{9}Be and ^{9}B have very weak B(GT) strengths, while transitions to the highly excited states have very large B(GT) strengths. This interpretation of the spatial structures of the A=9 nuclei and the strength of $\sigma\tau$-type transitions connecting them is illustrated in Fig. 6. The ground states of ^{9}Be and ^{9}B have a strongly deformed shape, which can be described in terms of a 2α+*particle* cluster model [46–48]. On the other hand, the ground states of ^{9}Li and ^{9}C, as well as their isobaric (highly excited) analog states in ^{9}Be and ^{9}B can be seen as more shell-model like due to their closed $p_{3/2}$ shells (for neutrons and protons, respectively) [7, 20].

The simultaneous description of states with strongly different spatial structures is a challenge for the shell model. While standard shell model calculations (see [36]) are able to predict quite well the excitation energies and B(GT) strengths leading to low-lying levels in ^{9}B, the higher excitation energies and B(GT) values could not be reproduced. A systematic shell model study of p-shell nuclei using a modified Hamiltonian (taking into account the role of the $j_>$-$j_<$, p-n monopole interaction) was undertaken by Suzuki, Fujimoto and Otsuka [49]. This study has yielded an improvement in the theoretical description of the GT strength distribution in the ^{9}Li β^- decay. Recent *ab initio* shell model calculations using a three-body interaction (TNI) [44, 45] have also been quite successful in the description of higher excited states in light nuclei. The small B(GT) strength of the ^{9}Li β^- decay to the ground state of ^{9}Be as well as the qualitatively larger B(GT) strength going to the higher excited states in ^{9}Be [similar to Fig. 5(b)] have also been reproduced in a recent cluster calculation using the AMD method [50].

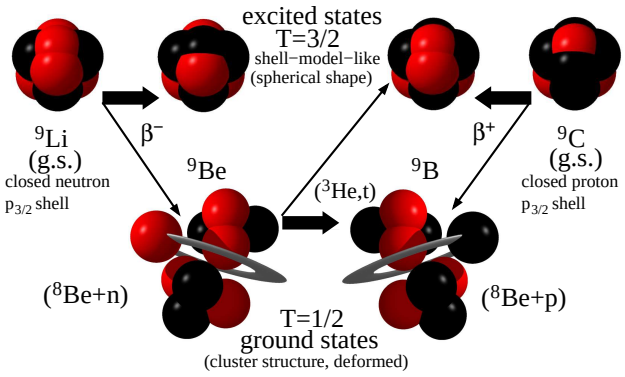

FIG. 6. (Color online) Illustration of the spatial shapes in the A=9 system and interpretation of the distribution of B(GT) strengths in charge-exchange processes in the A=9 system (see Figs 4 and 5). The ground states of ^{9}Li and ^{9}C can be considered spherical or mean-field-like, and have closed $p_{3/2}$ shells, while the ground states of ^{9}Be and ^{9}B are strongly deformed and have a 2α+n or 2α+p cluster structure. The weak process, mediated by the $\sigma\tau$ operator, connects states with very different spatial structure only very weakly. Transitions that have a large B(GT) value are marked with a thick arrow, while transitions with small B(GT) values are marked with a thin arrow.

VII. SUMMARY

We have measured the ^{9}Be(^{3}He,t)^{9}B reaction at 420 MeV beam energy (140 MeV/nucleon) and scattering angle around zero degrees. The high-resolution setup at the RCNP Osaka allowed to observe excited states in ^{9}B with an energy resolution of 30 keV. We determined excitation energies and decay widths of ^{9}B states up to 21 MeV. The angular distributions around zero degree scattering angle were obtained for these states (see table I) and it was found that ten states are excited by a $\Delta\ell$=0 transition (GT states). The excitation energy of the 16.8 MeV (5/2+) state was determined precisely, and its width was determined for the first time.

We determined the B(GT) strength of the $\Delta\ell$=0 transitions by using the proportionality [Eqs. (2) and (3)] between the differential cross-section at q=0 and the B(GT) strength (see Table III). The GT unit cross-section $\hat{\sigma}_{\rm GT}$ was determined using the data from analogous β decays of ^{9}Li and ^{9}C. The Fermi unit cross-section $\hat{\sigma}_{\rm F}$ was determined using the mass number systematics of the unit cross-sections [Eqs. (4), (5) and (14)].

The large difference between the B(GT) strengths for the transitions to the low-lying ^{9}B states and the ^{9}B states with higher energy point to a difference in spatial structures. This observation is corroborated by the B(GT) strengths derived from the β decays of ^{9}Li and ^{9}C. We also compared our experimental results to a previous (p,n) study, in which a determination of unit cross-sections [and thus B(GT) values] was not possible because of low resolution. We derived absolute B(GT) values from the given (p,n) cross-sections, and found that the values agree with our (^{3}He,t) data, but only for strong and well-separated states.

ACKNOWLEDGMENTS

The $(^3\mathrm{He}, t)$ experiments were performed at RCNP, Osaka University under the Experimental Program E273. The authors are grateful to the accelerator group of RCNP for providing a high-quality ^{3}He beam, and to the GSI target lab for the provisioning of the ^{9}Be target. This work was supported by the DFG, Germany under Contract Br799/13-1 and 20-1, MEXT, Japan under Grants No. 18540270 and No. 22540310, and the US NSF (PHY0216783 (JINA), PHY-0606007).

[1] F. Osterfeld, Rev. Mod. Phys. 64, 491 (1992).
[2] Y. Fujita, B. Rubio and W. Gelletly, Prog. Part. Nucl. Phys., In Press (2011).
[3] T.N. Taddeucci, C.A. Goulding, T.A. Carey *et al.*, Nucl. Phys. A 469, 125-172 (1987).
[4] Y. Fujita, K. Hatanaka, G.P.A. Berg *et al.* Nucl. Instr. and Meth. B 126, 274 (1997).
[5] T. Wakasa, K. Hatanaka, Y. Fujita *et al.*, Nucl. Instr. and Meth. A 482, 79-93 (2002).
[6] Y. Fujita, T. Adachi, H. Akimune *et al.*, Nucl. Phys. A 687, 311c (2001).
[7] Y. Fujita, Nucl. Phys. A 805, 408c (2008).
[8] J.C. Hardy and I.S. Towner, Phys. Rev. C 79, 055502 (2009).
[9] J.C. Hardy and I.S. Towner, Nucl. Phys. News 16, 11 (2006).
[10] W.E. Ormand and B.A. Brown, Phys. Rev. C 52, 2455 (1995).
[11] Y. Fujita, H. Akimune, I. Daito *et al.*, Phys. Rev. C 59, 90 (1999).
[12] Y. Fujita, Y. Shimbara, I. Hamamoto *et al.*, Phys. Rev. C 66, 044313 (2002).
[13] Y. Fujita, Y. Shimbara, A. F. Lisetskiy *et al.*, Phys. Rev. C 67, 064312 (2003).
[14] R.G.T. Zegers, H. Akimune, Sam M. Austin *et al.*, Phys. Rev. C 74, 024309 (2006).
[15] Y. Fujita, R. Neveling, H. Fujita *et al.*, Phys. Rev. C 75 057305 (2007).
[16] R.G.T. Zegers, T. Adachi, H. Akimune *et al.*, Phys. Rev. Lett.99, 202501 (2007).
[17] B.G. Pugh, Ph.D. thesis, Mass. Inst. Tech. (1985).
[18] A. Fazely, B. Anderson, A.R. Baldwin *et al.*, IUCF annual reports (1982), p. 49.
[19] H. Akimune, M. Fujimura, M. Fujiwara *et al.*, Phys. Rev. C 64, 041305(R) (2001).
[20] C. Scholl, Y. Fujita, T. Adachi *et al.*, AIP Conf. Proc. 1090, 544 (2009).
[21] I. Katayama, Chin. J. Phys. 27 (1989) 265.
[22] M. Fujiwara, H. Akimune, I. Daito *et al.*, Nucl. Instr. and Meth. A 422, 484-488 (1999).
[23] H. Fujita, Y. Fujita, G.P.A. Berg *et al.*, Nucl. Instr. and Meth. A 484, 17 (2002).
[24] A. Tamii *et al.*, IEEE Trans. Nucl. Sci. 43, 2488 (1996).
[25] W. Catford, program CATKIN, unpublished, http://personal.ph.surrey.ac.uk/∼phs1wc/kinematics/ (2004).
[26] D.R. Tilley, J.H. Kelley, J.L. Godwin *et al.*, Nucl. Phys. A 745, 155-362 (2004).
[27] H. Fujita, G.P.A. Berg, Y. Fujita *et al.*, Phys. Rev. C 79, 024314 (2009) and *priv. comm.*
[28] S. Dixit, W. Bertozzi, T.N. Buti *et al.*, Phys. Rev. C 43, 1758-1776 (1991).
[29] J. Cook and J.A. Carr, computer program FOLD, Florida State University (unpublished), based on F. Petrovich and D. Stanley, Nucl. Phys. A275, 487 (1977), modified as described in J. Cook et al, Phys. Rev. C30, 1538 (1984) and R.G.T. Zegers, S. Fracasso and G. Colo (2006), available online (http://www.nscl.msu.edu/∼zegers/fold.html).
[30] W.G. Love and M.A. Franey, Phys. Rev. C 24, 1073 (1981).
[31] M.A. Franey and W.G. Love, Phys. Rev. C 31, 488 (1985).
[32] N. Schwierz, I. Wiedenhöver and A. Volya, arXiv:0709.3525 [nucl-th], http://www.volya.net/ws (2008).
[33] S.Y. van der Werf, S. Brandenburg, P. Grasdijk *et al.*, Nucl. Phys. A 496, 305 (1989).
[34] L. Buchmann, E. Gete, J.C. Chow *et al.*, Phys. Rev. C 63, 034303 (2001).
[35] U.C. Bergmann, M.J.G. Borge, R. Boutami *et al.*, Nucl. Phys. A 692, 427-450 (2001).
[36] D. Mikolas, B.A. Brown, W. Benenson *et al.*, Phys. Rev. C 37-2, 766 (1988).
[37] G. Nyman, R.E. Azuma, P.G. Hansen *et al.*, Nucl. Phys. A 510, 189-208 (1990).
[38] Y. Prezado, U.C. Bergmann, M.J.G. Borge *et al.*, Phys. Lett. B 576, 55-61 (2003).
[39] S. Dangtip, J. Blomgren, N. Olsson *et al.*, Nucl. Phys. A 677, 3-24 (2000).

[40] Y. Fujita, B.A. Brown, H. Ejiri *et al.*, Phys. Rev. C 62, 044314 (2000).
[41] A.L. Cole, H. Akimune, S.M. Austin *et al.*, Phys. Rev. C 74, 034333 (2006).
[42] M. Ichimura, H. Sakai and T. Wakasa, Prog. Part. Nucl. Phys. 56, 446 (2006).
[43] Y. Fujita, P. von Brentano, T. Adachi *et al.*, Phys. Rev. C 70, 011306(R) (2004).
[44] P. Navratil, V.G. Gueorguiev, J.P. Vary *et al.*, Phys. Rev. Lett. 99, 042501 (2007).
[45] C. Forssen, P. Navratil, W.E. Ormand and E. Caurier, Phys. Rev. C 71, 044312 (2005).
[46] W. von Oertzen, Z. Phys. A 354, 37-43 (1996).
[47] W. von Oertzen, Z. Phys. A 357, 355-365 (1997).
[48] K. Arai, P. Descouvemont, D. Baye and W. Catford, Phys. Rev. C 68, 014310 (2003).
[49] T. Suzuki, R. Fujimoto and T. Otsuka, Phys. Rev. C 67, 044302 (2003).
[50] Y. Kanada-En'yo, Phys. Rev. C 81, 034321 (2010).